mDia2 regulates actin and focal adhesion dynamics and organization in the lamella for efficient epithelial cell migration

Stephanie L. Gupton[1], Kathryn Eisenmann[2], Arthur S. Alberts[2] and Clare M. Waterman-Storer[3,*]

[1]Department of Cell Biology, The Scripps Research Institute, La Jolla, CA 92037, USA
[2]Van Andel Research Institute, 333 Bostwick Avenue, Grand Rapids, MI 49503, USA
[3]Department of Cell Biology, The Scripps Research Institute, La Jolla, CA 92037, and Cell Biology and Physiology Center, National Heart, Lung and Blood Institute, Building 50 South Drive, Bethesda, MD 20892-8019, USA
*Author for correspondence (e-mail: watermancm@nhlbi.nih.gov)

Accepted 17 July 2007
Journal of Cell Science 120, 3475-3487 Published by The Company of Biologists 2007
doi:10.1242/jcs.006049

Summary

Cell migration requires spatial and temporal regulation of filamentous actin (F-actin) dynamics. This regulation is achieved by distinct actin-associated proteins, which mediate polymerization, depolymerization, severing, contraction, bundling or engagement to the membrane. Mammalian Diaphanous-related (mDia) formins, which nucleate, processively elongate, and in some cases bundle actin filaments, have been extensively studied in vitro, but their function in the cell has been less well characterized. Here we study the role of mDia2 activity in the dynamic organization of F-actin in migrating epithelial cells. We find that mDia2 localizes in the lamella of migrating epithelial cells, where it is involved in the formation of a stable pool of cortical actin and in maintenance of polymerization-competent free filament barbed ends at focal adhesions. Specific inhibition of mDia2 alters focal adhesion turnover and reduces migration velocity. We suggest that the regulation of filament assembly dynamics at focal adhesions may be necessary for the formation of a stable pool of cortical lamella actin and the proper assembly and disassembly dynamics of focal adhesions, making mDia2 an important factor in epithelial cell migration.

Supplementary material available online at
http://jcs.biologists.org/cgi/content/full/120/19/3475/DC1

Key words: FRAP, FSM, Adhesion, Depolymerization, Formin

Introduction

Cell migration consists of a polarized four step cycle of leading edge protrusion, adhesion to the extracellular matrix (ECM), forward contraction of the cell body, and release of adhesions in the cell rear (Lauffenburger and Horwitz, 1996). Each step of this cycle is mediated by distinct dynamic filamentous actin (F-actin) based structures. At the leading edge of migrating epithelial cells, F-actin is organized into two partially overlapping networks, the lamellipodium network and the lamella network (Gupton et al., 2005; Ponti et al., 2004). The distinct properties of F-actin in the two networks are probably dictated by the distribution and activities of actin-associated proteins that differentially associate with the networks (DesMarais et al., 2002; Ponti et al., 2004), conferring on each distinct functions for migration.

In the lamellipodium, which extends from the cell edge to ~2-4 μm into the cell, rapid polymerization and subsequent depolymerization of an F-actin array mediated by the Arp2/3 complex and cofilin (Arnaout, 2002; Bailly et al., 1999; Ichetovkin et al., 2002) produces a branched, treadmilling F-actin network. This network is pushed rapidly away from the cell edge by plasma-membrane-associated filament elongation (Pollard and Borisy, 2003; Ponti et al., 2004; Svitkina and Borisy, 1999) in a process termed retrograde flow. Cycles of filament polymerization and depolymerization within the treadmilling lamellipodium network correlate with cycles of leading edge protrusion and retraction (Machacek and Danuser, 2006; Ponti et al., 2004). A few micrometers behind the leading edge, F-actin in the lamella is organized into a network interspersed with bundles, both of which contain myosin II and tropomyosin (DesMarais et al., 2002; Gupton et al., 2005; Ponti et al., 2004; Verkhovsky et al., 1995). F-actin in the lamella undergoes myosin II-dependent retrograde F-actin flow that is slower than the polymerization-dependent flow of the lamellipodium (Ponti et al., 2004). Local sites of filament assembly and disassembly are intermingled throughout the lamella. Unlike the lamellipodium, it is unknown what proteins regulate the F-actin assembly and disassembly kinetics of the lamella.

Focal adhesions form at the interface between the lamellipodium and lamella F-actin networks (Ponti et al., 2004). Specific actin-binding proteins within focal adhesions may link F-actin in the lamella to transmembrane integrins (Critchley et al., 1999) that bind the ECM, stabilizing leading edge protrusions in the second step of migration. Myosin II contraction in the lamella, pulling on F-actin attached via focal adhesions to the ECM, generates tension for moving the cell body forward in the third step of migration (Lauffenburger and Horowitz, 1996). Actomyosin contraction is also implicated in the disassembly of trailing adhesions in the cell rear in the

final step of migration (Kaverina et al., 2002; Webb et al., 2004).

Recent studies have brought into question the role of the lamellipodium in cell migration (Pankov et al., 2005). Blocking lamellipodium formation by inhibiting the activity or expression of either Rac1 or Arp2/3 (Di Nardo et al., 2005; Gupton et al., 2005; Wheeler et al., 2006), or by mislocalizing Arp2/3 and cofilin (Gupton et al., 2005) demonstrated that loss of the lamellipodium does not inhibit migration velocity or directional persistence. Inhibition of lamellipodium formation in epithelial cells had no effect on F-actin dynamics or the overall structure and organization of F-actin in the lamella (Gupton et al., 2005). Taken together, these studies suggest that persistent leading edge advance and cell migration may be mediated by forward expansion of the lamella network (Gupton et al., 2005; Ponti et al., 2004) rather than with Arp2/3 and cofilin-mediated lamellipodium protrusion. Thus, elucidation of the molecular mechanism of cell motility requires understanding the regulation of F-actin in the lamella.

A candidate for regulating F-actin assembly in the lamella during cell migration is the diaphanous-related formin (DRF) protein family (Pruyne et al., 2002). Formins nucleate filaments from the fast-growing 'barbed' filament end, where they remain processively associated during elongation (Higashida et al., 2004; Kovar and Pollard, 2004; Romero et al., 2004). Formins change the kinetics of filament elongation by directing the addition of profilin-actin onto barbed ends at rates much faster than onto filaments without associated formins, and slow the rate of addition of G-actin without profilin onto filaments (Kovar et al., 2006; Romero et al., 2004). Formins also protect filament barbed ends from capping proteins and depolymerization (Harris and Higgs, 2006; Harris et al., 2004; Harris et al., 2006; Kovar et al., 2005; Moseley et al., 2004; Zigmond et al., 2003). Additionally, some formins can bundle or sever F-actin in vitro (Harris et al., 2004; Michelot et al., 2005). Formin family proteins are located throughout the cell on both F-actin and microtubule structures, as well as on endosomes and mitochondria (Eisenmann et al., 2005; Palazzo et al., 2001; Tominaga et al., 2000; Wallar et al., 2007; Watanabe et al., 1999). Although they act as effectors for Rho family small GTPases, the DRFs mDia1 and mDia2 have been shown to mediate assembly of F-actin in stress fibers and filopodia in various cell types (Hotulainen and Lappalainen, 2006). However, little is known about the function of mDias in the lamellipodium and lamella F-actin networks of epithelial cells, and how these functions contribute to the ability of these cells to migrate.

Here we sought to determine the role of DRFs in the spatial regulation of F-actin dynamics in lamellipodium and lamella of migrating PtK1 epithelial cells that typically do not exhibit stress fibers or filopodia, yet express mDia2. Our results indicate that mDia2 localizes in the central cell area and lamella, but is absent from the lamellipodium actin meshwork, suggesting a role in F-actin dynamics in the lamella. By microinjecting antibodies that specifically inhibit mDia2-mediated F-actin polymerization, we find that mDia2 maintains a stable pool of cortical F-actin in the lamella and plays a role in the turnover of focal adhesions, where it maintains polymerization-competent free barbed filament ends. The regulation of F-actin in the lamella by mDia2 is critical in cell migration, as mDia2 inhibition reduces cell migration velocity.

Results

mDia2 localizes to the cell center and lamella, but not to the lamellipodium

Since studies on DRF protein function have solely focused on filopodia or stress fibers in non-epithelial cell types, we focused on the role of DRFs in the spatiotemporal regulation of actin-mediated processes in migrating PtK1 epithelial cells, which typically do not exhibit filopodial protrusions or stress fibers. We have previously characterized migration of these cells, as well as the kinetics (turnover) and kinematics (movement) of their actin cytoskeleton dynamics (Gupton et al., 2005; Gupton and Waterman-Storer, 2006b; Ponti et al., 2004; Wittmann et al., 2003), making them ideal for determining DRF protein function in lamellipodial and lamella F-actin behavior and cell migration. The DRF family has three members: mDia1, mDia2 and mDia3 (Higgs and Peterson, 2005). We first determined the expression and localization of these members in PtK1 cells. Immunoblotting PtK1 cell lysates revealed that these cells did not express detectable mDia1, but expressed both mDia2 and mDia3 (Fig. 1A-C). Immunoprecipitation and western blotting of cell lysates with antibodies specific to mDia3 followed by blotting the immunoprecipitate with antibodies against mDia2 showed no cross-reactivity of the anti-mDia2 antibodies with the more abundant mDia3 (data not shown). mDia3 is thought to function in spindle pole alignment (Yasuda, 2003) and/or endosomal dynamics (Ridley, 2006; Gasman, 2003; Yasuda, 2003). Therefore, we chose to focus on the contributions of mDia2 towards leading edge F-actin dynamics in PtK1 cells.

To determine the localization of mDia2 in PtK1 cells, we used immunofluorescence and expressed GFP-fusion protein. Immunolocalization of endogenous mDia2 in fixed cells revealed diffuse mDia2 throughout the cell, as well as vesicular and filamentous staining in all cellular regions except near the cell leading edge (Fig. 1D-G, supplementary material Fig. S1A). To determine the nature of the diffuse mDia2 staining, cells were extracted and fixed with methanol (supplementary material Fig. S1B). This also revealed a vesicular and filamentous staining of mDia2 in the cell center and lamella region, but a loss of the diffuse staining. Expression of mDia2-eGFP fusion protein and visualization by either confocal or total internal reflection fluorescence (TIRF) microscopy showed diffuse localization of mDia2 throughout the cell (by confocal) and on the ventral 100 nm of the cell (by TIRF; supplementary material Fig. S1C,D). Thus, mDia2 localizes to insoluble structures that are absent from the cell edge.

We next determined the cytoskeletal structures with which mDia2 was associated by colocalization. Fluorescent phalloidin staining revealed no mDia2 colocalization on the dense F-actin network at the front few micrometers of the cell in the region corresponding to the lamellipodium (Fig. 1D). In addition, mDia2 did not colocalize at the leading edge with the lamellipodium signature protein, Arp3 (Fig. 1E). Rather, the filamentous mDia2 extended from the cell center into the lamella, where the lamella signature protein, phosphoserine-19 myosin II regulatory light chain (pMLC), indicative of activated myosin II, was also concentrated (Fig. 1F). Co-

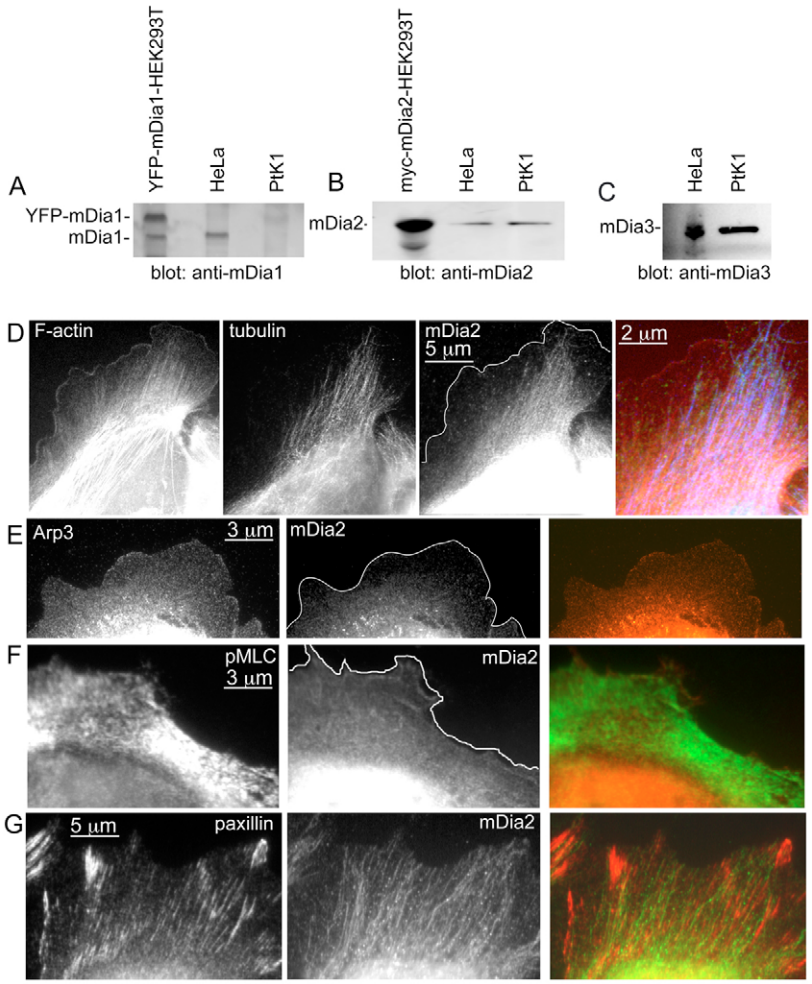

Fig. 1. PtK1 cells express mDia2, which localizes in the lamella and cell center and not to the lamellipodium. Whole cell lysates from HEK 293T cells expressing either YFP-fused mDia1 (A) or Myc-tagged mDia2 (B), as well as HeLa and Ptk1 cell lysates (A-C) were prepared. Lysates were immunoblotted with antibodies directed against mDia1 (A), mDia2 (B), or mDia3 (C). (D) Fluorescent phalloidin staining of F-actin and immunofluorescence of tubulin and mDia2. In the merged image, tubulin is blue, mDia2 is green, and F-actin is red. mDia2 partially colocalizes with microtubules in the lamella and is excluded from near the cell edge. The cell edge as determined from phase-contrast images (not shown) is outlined in white in this and subsequent images. (E) Immunofluorescent staining for Arp3 and mDia2 in PtK1 cells. In the merged image, Arp3 is in red, and mDia2 is in green. Arp3 concentrates in a thin band along the cell edge in the lamellipodium where mDia2 is depleted. (F) Immunofluorescent staining for myosin II regulatory light chain phosphorylated at Ser-19 (pMLC) and mDia2. Merged image shows pMLC in red and mDia2 in green. mDia2 is present in the lamella where pMLC is concentrated. (G) Paxillin and mDia2 immunofluorescence, paxillin in red, mDia2 is in green. mDia2 and paxillin do not colocalize.

labeling with tubulin antibodies revealed colocalization with a subset of microtubules (Fig. 1D), in agreement with a previous study (Palazzo et al., 2001). Co-labeling with paxillin antibodies (Fig. 1G) showed no obvious colocalization of mDia2 with focal adhesions. Thus, in epithelial cells, mDia2 associates with microtubules and other insoluble structures in the lamella and cell center, but is absent from the lamellipodium.

mDia2 antibody inhibits mDia2-mediated F-actin polymerization

To determine if mDia2 is involved in the regulation of F-actin dynamics, we sought to perturb mDia2 function by antibody inhibition. We used a specific polyclonal antibody raised against the FH2 domain of murine mDia2 (Fig. 1) (Peng et al., 2003; Wallar et al., 2007), as this domain is critical to the actin regulatory functions of Dia proteins. Monitoring the fluorescence of pyrene-labeled actin by in vitro polymerization assays using purified proteins indicated that this antibody inhibited actin polymerization mediated by the FH1FH2 domains of mDia2 but not by the FH1FH2 domains of mDia1 (supplementary material Fig. S2) (Wallar et al., 2007). Microinjection of this antibody into mouse embryonic fibroblasts previously showed disruption of actin bundles and filopodia (Peng et al., 2003). When microinjected into PtK1 cells, the localization of this antibody was indistinguishable from that of GFP-mDia2 fusion protein, as determined by immunofluorescence (supplementary material Fig. S1).

mDia2 maintains a stable pool of F-actin in the lamella

To determine the role of mDia2 activity in F-actin dynamics in migrating epithelial cells, we inhibited mDia2 by microinjection of 0.1 mg/ml of the inhibitory mDia2 antibody into PtK1 cells migrating at the edge of epithelial cell islands in tissue culture. To visualize F-actin, cells were microinjected with X-Rhodamine-labeled actin either alone or together with the inhibitory mDia2 antibody. To assay F-actin dynamics in the ventral cortex of cells, we used total internal reflection fluorescence recovery after photobleaching (TIR-FRAP) (Sund and Axelrod, 2000). FRAP of fluorescent actin in the ventral cell cortex using TIRF microscopy allows quantification of the rate and completion of fluorescence recovery, indicating how quickly fluorescent actin in the cortex cycles between the cytoskeleton-bound and cytoplasmic pools. A strong evanescent excitation field was introduced within 150 nm of the coverslip-cell interface by a pulse of 568 nm laser light at a critical angle to specifically bleach fluorescent actin incorporated into the ventral cortical cytoskeleton without bleaching the bulk of fluorescent actin in the cytosol (Fig. 2; supplementary material Movie 1). However, since the lamella and lamellipodia of PtK1 cells is 80-120 nm thick (AFM measurements; M. Gardel and K. VanVleit and C.M.W.-S., unpublished observations) this technique photobleaches most of the fluorescent actin within these two structures. Following photobleaching, fluorescence recovery was imaged at 1-5 second intervals using TIRF microscopy with laser illumination at a much lower power.

We analyzed fluorescence recovery in the lamellipodium and lamella to determine if mDia2 differentially regulates

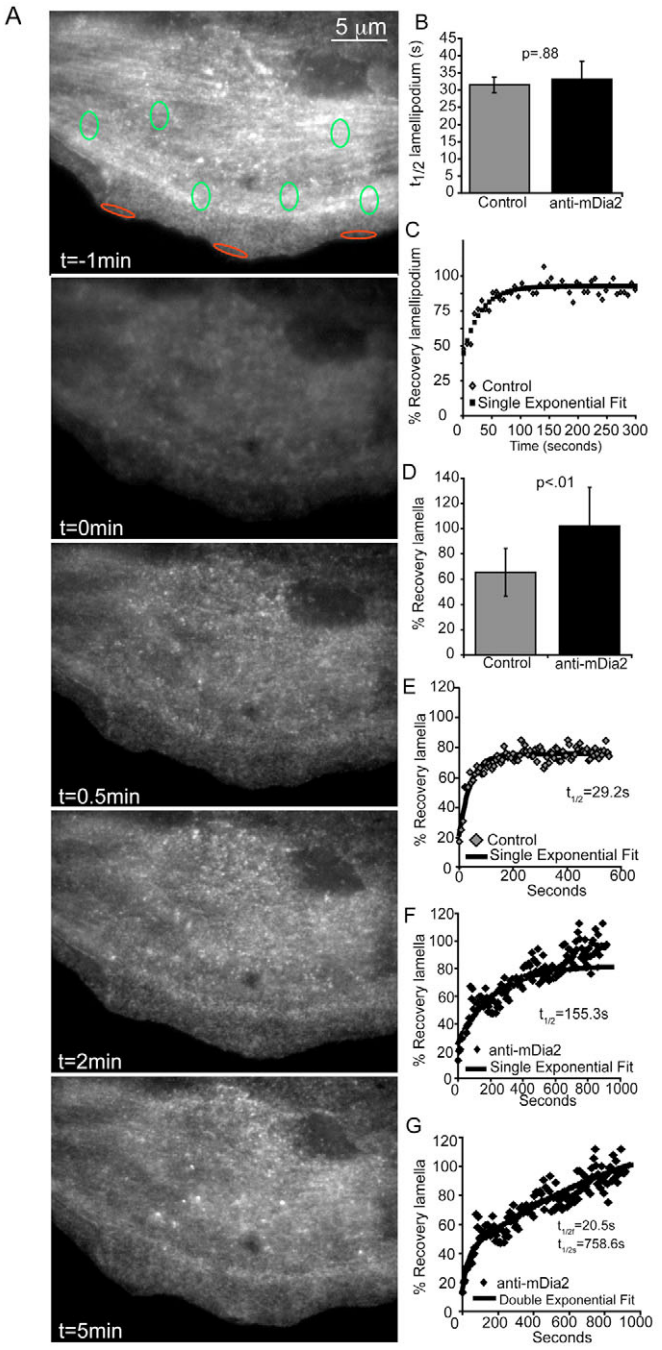

Fig. 2. mDia2 forms a stable pool of cortical actin in the lamella. (A) Example of a TIR-FRAP experiment; X-Rhodamine actin TIRF images taken from a time-lapse movie of a PtK1 control cell prior to and after fluorescence photobleaching of ~150 nm of the ventral cell cortex, which occurs at t=0. Lamellipodium measurements were taken at the extreme cell edge (red ovals). Green ovals indicate regions where fluorescence intensity measurements were taken in the lamella. (B) $t_{1/2}$ of fluorescence recovery of F-actin in the lamellipodium of control (n=5) and mDia2 antibody (anti-mDia2, n=5) -injected cells. (C) Example of actin fluorescence recovery data (diamonds) fit to a single term exponential (squares) in the lamellipodium of a control PtK1 cell. (D) Percentage of fluorescence recovery after photobleaching of F-actin in the lamella of control (n=5) and mDia2 inhibited cells (n=5, ± s.d.). mDia2 antibody inhibition mobilizes a stable, non-recovering pool of fluorescent actin. (E,F) Examples of fluorescence recovery data (diamonds) fit to a single term exponential (black line) obtained from the lamella of (E) a control PtK1 cell and (F) an mDia2 antibody-injected cell. (G) Data from F (diamonds) fit to a two-term exponential (black line), revealing that F-actin in the lamella of mDia2 antibody-injected cells has a different mechanism of fluorescence recovery than controls, in which the data was fit by a single exponential.

these F-actin structures. These regions were distinguished by their typical differences in F-actin retrograde flow velocities and location relative to the leading cell edge (Ponti et al., 2004; Salmon et al., 2002). Analysis of the lamellipodium at the cell edge (red ovals, Fig. 2A) indicated that in both control and mDia2-inhibited cells, fluorescence recovery after bleaching was complete (indicated by percentage of recovery, Fig. 2C and data not shown) and occurred at similar rates (indicated by the half-time of recovery $t_{1/2}$, Fig. 2B). In contrast, analysis of fluorescent actin in the lamella (green ovals, Fig. 2A) revealed differences between control and mDia2-inhibited cells (Fig. 2D-G). Fluorescence recovery in the lamella of control cells fit to a single exponential curve with a $t_{1/2}$ of 26.1±0.9 seconds, but was incomplete within the 600-1000 seconds duration of experiments (65.4±2%; Fig. 2D,E). This suggests that F-actin in the lamella of control cells resides in two distinct pools: a dynamic pool that recovered fluorescence in minutes by one mode of actin turnover noted by the single exponential fit, and a more stable pool that did not turn over within ~20 minutes, noted by the incomplete fluorescence recovery. Unlike control cells, F-actin fluorescence in the lamella of mDia2-inhibited cells fully recovered after bleaching, indicating that all F-actin in the lamella was dynamic (P<0.0001, Mann-Whitney test; Fig. 2D). In addition, fluorescence recovery did not fit a single exponential (Fig. 2F), but rather a two-term exponential (Fig. 2G), suggesting two overlapping mechanisms of F-actin turnover. Whereas one phase of recovery was faster than in control cells ($t_{1/2}$=12.5±0.6 seconds; P<0.0001) the other phase was significantly slower ($t_{1/2}$=739±92.6 seconds, P<0.0001).

Thus, mDia2 is not involved in the turnover of F-actin in the lamellipodium, but rather functions in F-actin dynamics in the lamella. Furthermore, this data indicates there are both stable and dynamic pools of F-actin in the lamella of migrating epithelial cells, and that mDia2 activity is necessary for the formation or maintenance of the stable F-actin pool, and may also slow the turnover of the dynamic pool.

mDia2 inhibition alters the kinematics and kinetics of F-actin in cells

We next sought to investigate the role of mDia2 in the spatial organization of F-actin assembly, disassembly, and motion dynamics in migrating epithelial cells. To achieve this, control and mDia2-inhibited cells were subjected to fluorescent speckle microscopy (FSM) imaging of microinjected X-Rhodamine actin and quantitative analysis of FSM time-lapse movies (qFSM) (supplementary material Movie 2) (Danuser and Waterman-Storer, 2003). Whereas TIR-FRAP provides absolute measures of the rate of F-actin dissociation from the cytoskeleton, qFSM computer vision software can track the position and intensity fluctuations of fluorescent F-actin speckles over time to produce high-resolution spatiotemporal

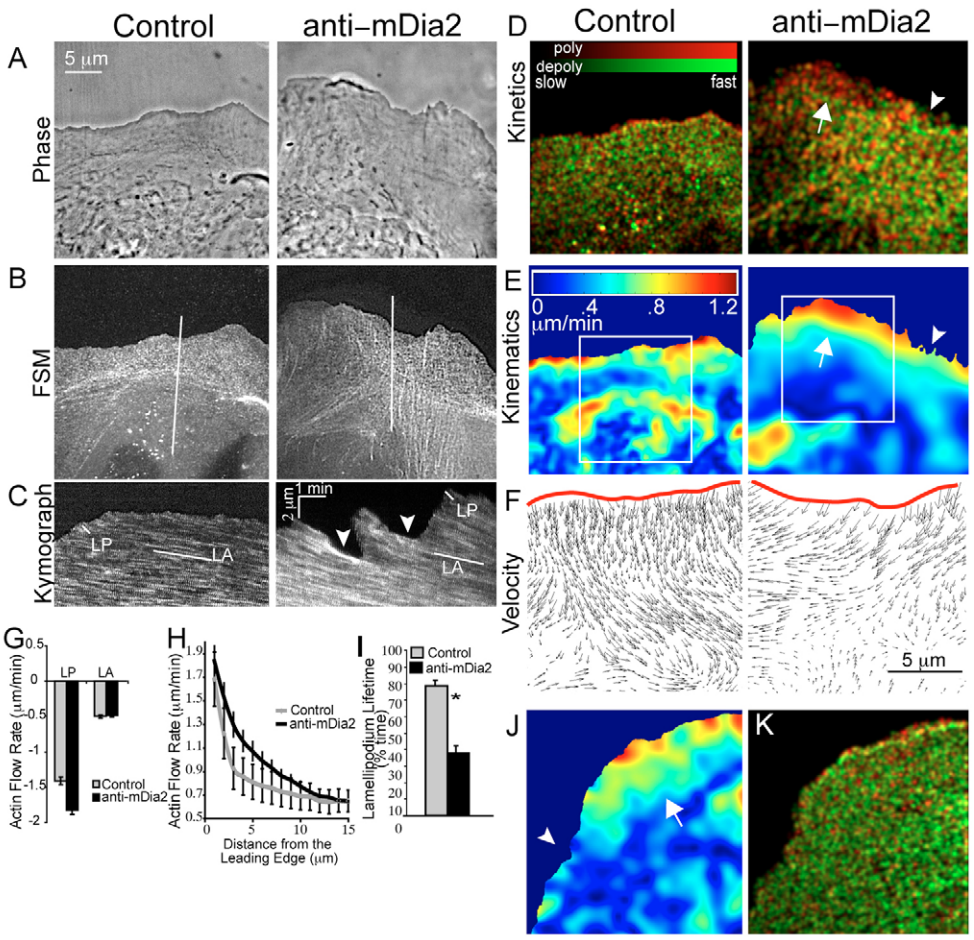

Fig. 3. mDia2 is necessary for the segregation of distinct dynamic F-actin behavior of the lamellipodium and lamella. Phase-contrast (A) and FSM (B) images of X-Rhodamine actin in control and mDia2 antibody-injected (anti-mDia2) cells. (C) Kymographs taken along the axis of F-actin flow, indicated by the lines in B. Three kymographs were taken from each of five cells per treatment for the analyses shown in G and I. In C, lines indicate the F-actin speckle flow rate in the lamellipodium (LP) and lamella (LA); arrowheads indicate lack of the rapid retrograde flow typical of the LP. (D) qFSM maps of F-actin polymerization (red) and depolymerization (green) rates in control and mDia2 antibody-injected (anti-mDia2) cells. Brightness indicates the relative magnitude of the rate. The arrow indicates a wide region of rapid F-actin polymerization along the cell edge (LP), and the arrowhead indicates a region of no rapid F-actin polymerization at the cell edge (no LP). (E) qFSM maps of the speed of F-actin flow in control and mDia2 antibody-injected (anti-mDia2) cells; the arrow indicates a shallow speed gradient. The arrowhead indicates a region of no rapid retrograde flow at the cell edge. (F) qFSM speckle velocity from regions indicated by boxes in E. (G) Average rates of F-actin retrograde (–) or anterograde flow (+) in the LP and LA, determined from kymographs of FSM movies (± s.e.m.). (H) Rate of F-actin flow as a function of distance from the cell edge in control and anti-mDia2 antibody injected cells. F-actin flow speed at all points in the cell, as determined by qFSM, was averaged parallel to the cell edge in 1 μm intervals behind the cell edge for five control and anti-mDia2 antibody-injected cells. (± s.e.m.). (I) Percentage of time in which fast flow of lamellipodium was present, as analyzed from kymographs (± s.e.m.). The asterisk in I indicates statistical significance ($P<0.05$) between control and mDia2 antibody-injected cells. (J,K) qFSM maps of (J) the speed of F-actin flow and (K) of F-actin polymerization (red) and depolymerization (green) rates in a PtK1 cell expressing a dominant negative FH2 (δFH2) construct.

maps of F-actin speed and direction (kinematics) and local relative rates of F-actin polymerization and depolymerization (kinetics) (Ponti et al., 2005; Ponti et al., 2003).

In control cells, qFSM analysis revealed the characteristic segregation of F-actin into distinct lamellipodium and lamella networks (Ponti et al., 2004). In kinematic maps and kymographs, the lamellipodium was typified by fast (~1.5 μm/minute) F-actin retrograde flow in a band approximately 2 μm wide at the leading cell edge (Fig. 3C,E in red). This fast-flow band spatially corresponded with a narrow band of rapid polymerization along the cell edge seen in the kinetic maps (red, Fig. 3D) (Ponti et al., 2004). In the region proximal to the lamellipodium, F-actin exhibited lamella signature kinematics and kinetics, characterized by slow retrograde flow (~0.5 μm/minute; Fig. 3F, and green-cyan region in Fig. 3E) and intermixed foci of rapid polymerization and depolymerization (Fig. 3D). The interface between the lamellipodium and lamella was delineated by a sharp gradient in F-actin flow speed that occurred about 2 μm from the cell edge, as seen in the kymograph in Fig. 3C, and in the speckle speed maps as a narrow area near the cell edge in which F-actin speed abruptly slowed from over 1.2 μm/minute (red) to ~0.4 μm/minute (cyan, Fig. 3E).

FSM analysis revealed subtle yet consistent differences in the organization of F-actin kinematics and kinetics in cells injected with the mDia2 antibody. mDia2 inhibition had no effect on the general location of the lamellipodial and lamella networks, nor on the average rates of F-actin retrograde flow in these regions (Fig. 3G). However, examination of kymographs and qFSM maps suggested that mDia2-inhibited cells often temporarily lacked the region of fast retrograde flow and rapid polymerization at sites along the cell edge, suggesting local loss of the lamellipodium (Fig. 3C-E arrowheads). By measuring the time in which a region of fast flow at the cell edge, i.e. a lamellipodium, was present in kymographs, we found that in mDia2-inhibited cells, the lamellipodium only existed 40% of time, whereas in control cells a lamellipodium was present more than 80% of the time

(Fig. 3I). In addition, qFSM maps suggested that when a lamellipodium was present in mDia2 antibody-injected cells, there was a distinct broadening of the interface between the lamellipodium and lamella. In kinematic maps the broadening of this interface was seen as the color change from red at the leading edge to cyan-blue in the lamella, which occurred over a wider area in mDia2-inhibited cells than in control cells (Fig. 3E arrow). This indicated a shallow actin flow speed gradient, compared to the sharp speed gradient seen in control cells. Indeed, statistical analysis of the average rate of retrograde flow versus distance behind the leading edge showed that mDia2 inhibition induced a shallower speed gradient (Fig. 3H, n=5 cells per treatment). In kinetic maps of mDia2-inhibited cells, the band of rapid polymerization (red) followed by rapid depolymerization (green) was expanded over a wider area compared to controls (Fig. 3D, arrows and arrowheads respectively).

To confirm the effects of the mDia2 antibody inhibition, we expressed an FH2 domain construct of mDia1 containing dominant negative mutations (δFH2) (Copeland and Treisman, 2002), that has previously been shown to block both mDia1 and mDia2-mediated functions in the actin cytoskeleton (Copeland et al., 2004; Copeland and Treisman, 2002). Expression of this dominant negative construct caused changes in F-actin kinematics typified by a broadening of the F-actin retrograde flow speed gradient at the cell edge (Fig. 3J), similar to the kinematic phenotype seen with mDia2 antibody inhibition. Similarly, sites along the cell edge often lacked regions of fast F-actin flow and rapid polymerization (Fig. 3J-K, arrowheads), suggesting the loss of a lamellipodium. However, in other sites along the cell edge, the bulk of actin polymerization was still concentrated at the leading edge, and not spread out over the width of the fast flow region, as was seen in anti-mDia2 antibody-inhibited cells. The reason for this difference between the antibody inhibition and δFH2 expression is unclear, but could be due to the δFH2 interfering with other formins in the cell.

Together, analysis of the spatial organization of F-actin dynamics by qFSM indicates mDia2 plays a role in maintaining the stability of the lamellipodium and segregation of F-actin kinematics and kinetics between the lamellipodium and lamella. The melding of lamellipodium and lamella in mDia2-inhibited cells could also underlie the increase in F-actin turnover as measured by TIR-FRAP in what was presumed, based on F-actin retrograde flow speed in those experiments, to be the lamella region.

mDia2 mediates proper focal adhesion distribution

We have shown previously that the distal edge of focal adhesions lie at the lamellipodium-lamella interface (Ponti et al., 2004; Hu et al., 2007). Since mDia2 inhibition specifically affected this interface, this suggested mDia2 may regulate focal adhesion behavior. To test this, we inspected the distribution of focal adhesions in control, anti-mDia2 antibody-injected cells, and cells expressing the dominant negative δFH2 construct (Fig. 4). In control cells, paxillin immunofluorescence and GFP-paxillin expression showed that large focal adhesions localized primarily at the cell periphery, a few micrometers from the leading edge, previously shown to be the lamellipodium/lamella interface. In contrast, in anti-mDia2 antibody-injected cells and δFH2 expressing cells, there were a significantly increased number of paxillin-containing focal adhesions localized throughout the lamella, which were smaller than in control cells (Fig. 4C,D). Microinjection of a similar anti-mDia1 antibody (Tominaga et al., 2000) at a concentration of 0.1 mg/ml into PtK1 cells did not produce the same changes in focal adhesion size and distribution as did the mDia2 antibody (Fig. 4). This suggests that the effects of mDia2 antibody or dominant negative perturbation were specific.

Together, the widening of the zone of focal adhesions in mDia2 inhibited cells suggests that mDia2 may maintain the segregation of the lamellipodium and lamella through effects on focal adhesion distribution, or vice versa.

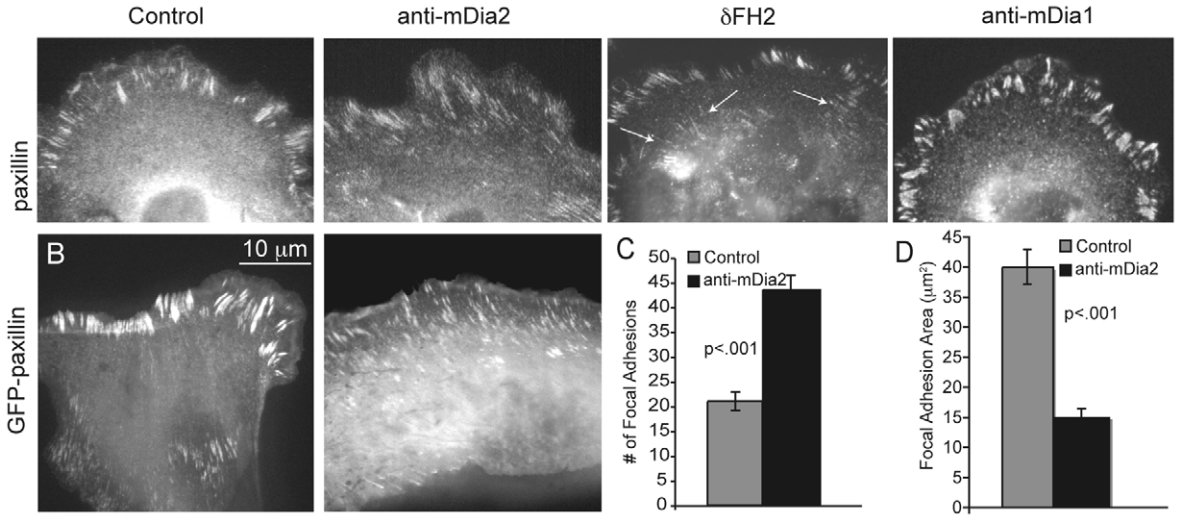

Fig. 4. mDia2 is necessary for normal focal adhesion morphometry. (A) Paxillin immunofluorescence in control, mDia2 antibody-injected (anti-mDia2), dominant negative mutant expressing (δFH2), and mDia1 antibody-injected (anti-mDia1) cells. (B) Control and mDia2 antibody-injected cells expressing GFP-paxillin. (C,D) Average number per cell (C), and size (D) of paxillin stained focal adhesions ± s.e.m., n=12 cells per treatment.

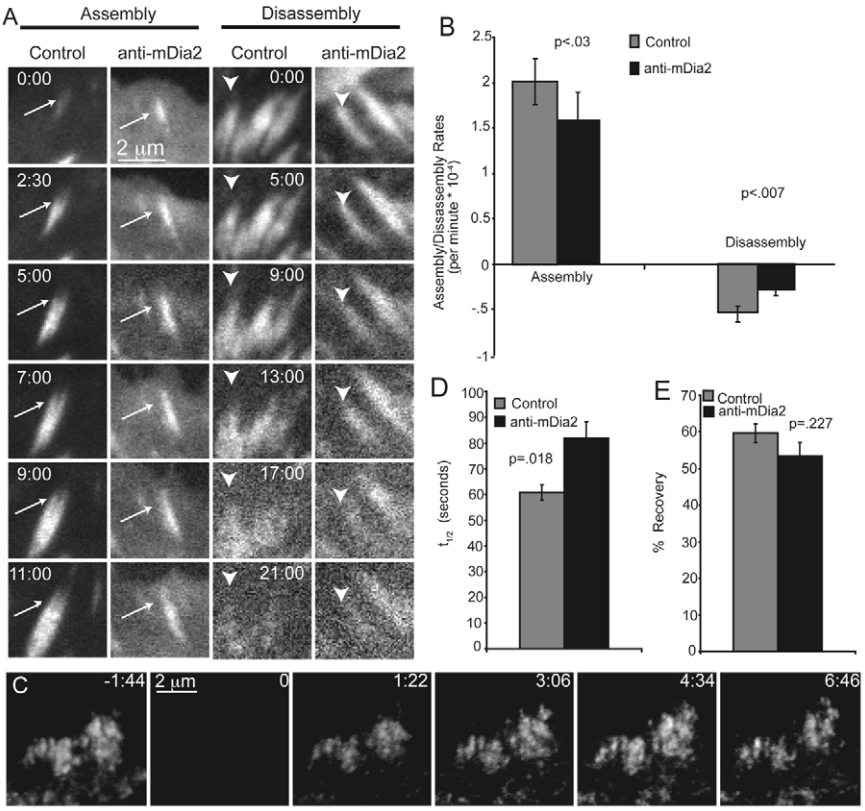

Fig. 5. mDia2 is necessary for normal focal adhesion dynamics. (A) Example of focal adhesion dynamics seen in frames from a time-lapse spinning disk confocal microscopy image series of GFP-paxillin in control and anti-mDia2 antibody-injected cells, arrows and arrowheads indicate focal adhesion assembly and disassembly respectively. (B) The average rate constants of FA assembly and disassembly measured from 5-20 focal adhesions per cell in four to five cells per condition (± s.d.). (C) Example of a TIRF-FRAP experiment; GFP-paxillin TIRF images were taken from a time-lapse of a PtK1 cell prior to and after fluorescence photobleaching of the ventral cell cortex, which occurs at t=0. (D) $t_{1/2}$ of fluorescent recovery after photobleaching of GFP-paxillin in focal adhesions in control and mDia2 antibody-injected cells, n=5 cells per treatment. (E) Percentage of fluorescent recovery after photobleaching of GFP-paxillin in focal adhesions in control and mDia2 antibody-injected cells.

mDia2 promotes focal adhesion turnover

The increase in focal adhesion number across the lamella induced by mDia2 inhibition suggests that mDia2 may function to regulate focal adhesion dynamics, as has been shown for the related DRF, mDia1, in rat glioma cells (Yamana et al., 2006). To determine if focal adhesion activity was affected by mDia2 inhibition, GFP-paxillin was imaged over time in control and anti-mDia2 antibody-injected cells by time-lapse spinning-disk confocal microscopy (supplementary material Movie 3; Fig. 5A). In control cells, small focal adhesions formed behind the leading edge during forward cell edge protrusion (Fig. 5A, arrows). As new focal adhesions formed, older focal adhesions more distal from the leading edge disassembled (Fig. 5A, arrowheads), as previously observed (Gupton and Waterman-Storer, 2006a; Laukaitis et al., 2001). In anti-mDia2 antibody-injected cells, focal adhesions still formed a few microns behind the leading edge, but failed to disassemble as the cell edge advanced away from them (supplementary material Movie 3). Only a few focal adhesions in these cells ever disassembled during the 45 minutes of imaging, indicating mDia2 antibody inhibition increased focal adhesion lifetime. To test if mDia2 function affected focal adhesion assembly or disassembly rates, we measured the rate of GFP-paxillin intensity increase or decrease in forming or disassembling focal adhesions in the lamella of control and mDia2-inhibited cells (Fig. 5B) as performed by Webb et al. (Webb et al., 2004). mDia2 inhibition slowed the rate of focal adhesion assembly by approximately 25% (P<0.03), and retarded the rate of focal adhesion disassembly by ~50% (P<0.007, Mann-Whitney test).

Focal adhesion proteins constantly exchange between cytoplasmic and membrane-associated pools (Zaidel-Bar et al., 2003; Zimerman et al., 2004). To determine if this cycling was affected by mDia2 inhibition, we performed TIR-FRAP experiments on the ventral 150 nm cortex of cells expressing GFP-paxillin, and imaged fluorescence recovery using TIRF microscopy (Fig. 5C). In both control and mDia2 antibody-injected cells, paxillin fluorescence recovery in focal adhesions fit to a single exponential curve, with adhesions in both types of cells recovering approximately 60% of their initial fluorescence (Fig. 5D, P=0.23). This indicates that focal adhesions in PtK1 cells have both a mobile and immobile pool of paxillin and partitioning of these fractions is unaffected by mDia2 function. However, fluorescence recovery of GFP-paxillin in the mobile pool was significantly slower in anti-mDia2 antibody-injected cells ($t_{1/2}$=76.5 seconds, n=12-15 adhesions in four cells each) compared with control cells ($t_{1/2}$=58.9 seconds, P<0.02, 10-12 adhesions in five cells each; Fig. 5E), indicating a slower dissociation of paxillin from focal adhesions, in agreement with a slowed disassembly rate.

These data show that mDia2 function is necessary for the normal assembly-disassembly cycle of focal adhesions and that its inhibition slows both assembly and disassembly, which may be mediated by a slowing of the cycling of proteins between focal adhesions and the cytosolic pool. Decreased rates of adhesion disassembly may cause the build-up of centrally located focal adhesions seen in anti-mDia2 antibody-injected cells.

mDia2 maintains polymerization-competent free filament barbed ends at focal adhesions

It has recently been shown that the DRF mDia1 promotes the

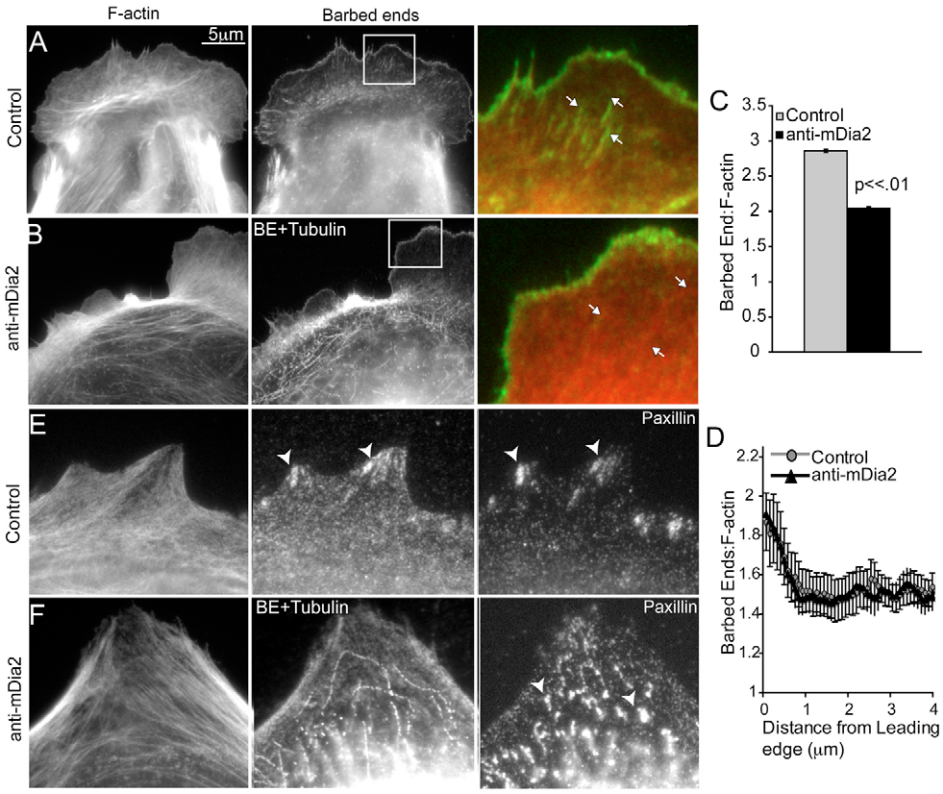

Fig. 6. mDia2 maintains free filament barbed ends at focal adhesions. Barbed-end actin incorporation (green) and fluorescent phalloidin staining of F-actin (red) in a control cell (A) and mDia2 antibody-injected cell (anti-mDia2; B). To find mDia2 antibody-injected cells after permeabilization, mDia2 antibody was co-microinjected with fluorescent tubulin that can be seen incorporated into microtubules that are easily distinguishable from actin structures. Arrows indicate plaques at the termini of actin bundles (arrowheads). (C) Intensity ratio of fluorescent actin incorporation marking free barbed filament ends relative to total F-actin (phalloidin) at the terminal 2 μm of actin bundles (n=10 cells per treatment, ~5-10 bundles/cell). (D) Intensity ratio of fluorescent actin incorporation marking free barbed filament ends relative to total F-actin (phalloidin) (± s.e.m.) from the leading-edge into the cell center is not altered by αmDia2 inhibition, n=10 cell per treatment, three regions per cell. (E,F) Fluorescent phalloidin, barbed-end actin incorporation, and paxillin immunofluorescence in a control cell (E) and an mDia2 antibody-injected cell (F). In a control cell, actin incorporates at focal adhesions that are positive for paxillin (arrowheads), but this does not occur in mDia2 antibody-injected cells. Note the altered focal adhesion morphology in cells injected with mDia2 antibody as seen by paxillin immunofluorescence (F), suggesting that antibody inhibition renders focal adhesions labile to the pre-permeabilization procedure required for localization of free barbed ends.

assembly of F-actin at focal adhesions to mediate the formation of dorsal stress fibers in U2OS human osteosarcoma cells (Hotulainen and Lappalainen, 2006). This together with our observations on the effects of mDia2 on actin and focal adhesion dynamics suggested that mDia2 may also regulate actin assembly specifically at focal adhesions. To test this hypothesis in PtK1 cells where stress fibers are not common, we used an assay to localize polymerization-competent free barbed ends at focal adhesions in control and mDia2-inhibited cells (Symons and Mitchison, 1991). Cells were permeabilized in the presence of low levels of fluorescent actin under conditions that allow actin polymerization only at uncapped barbed filament ends, followed by fixation and staining with spectrally distinct fluorescent phalloidin to visualize total F-actin (Fig. 6). The ratio of fluorescence of polymerized F-actin to phalloidin staining then reveals the relative amount of free filament barbed ends available for polymerization locally in the cell.

In control cells, filament free barbed ends localized along the leading edge of the lamellipodium (Fig. 6A) as previously shown (Bailly et al., 1999; Symons and Mitchison, 1991), and prominently to plaques at the termini of thin F-actin bundles (Fig. 6A, arrows), which probably corresponded to focal adhesions. When paxillin was colocalized in cells with fluorescent actin incorporation, plaques of free barbed ends colocalized with plaques of paxillin immunofluorescence (Fig. 6E), confirming localization of free barbed ends to focal adhesions. In cells in which mDia2 antibody was microinjected, there were differences in the amount and localization of free filament barbed ends. In order to identify anti-mDia2 antibody-injected cells after extraction for the actin incorporation assay, cells were co-microinjected with antibody and fluorescently labeled tubulin that assembled into the insoluble microtubule cytoskeleton. mDia2 antibody-injected cells showed similar incorporation of fluorescent actin at barbed ends along the leading edge as uninjected controls (Fig. 6B,D). However, in contrast to control cells, mDia2 inhibition caused a 30% reduction in the amount of free barbed ends at the termini of thin F-actin bundles (Fig. 6B, arrows, 6C, P<0.0001). Co-staining free barbed ends and paxillin confirmed that inhibition of mDia2 by antibody microinjection reduced fluorescent actin incorporation at focal adhesions (Fig. 6F). Also, focal adhesion distribution and morphology appeared to be altered in these cells, as seen by an increase in the number of focal adhesions (Fig. 4), which were long and appeared clumpy relative to focal adhesions in control cells. Since microinjected mDia2 antibody did not alter focal adhesion morphology, as seen by GFP-paxillin localization in live cells and immunofluorescence of endogenous paxillin in cells fixed before permeabilization (see Fig. 4), it is possible that injected mDia2 antibodies make focal adhesions unstable to the pre-permeabilization before fixation procedure that is required for localizing free barbed ends. Together, these data suggest mDia2 is necessary for free barbed filament end formation or maintenance at focal adhesions in the lamella, but not at the leading edge of the lamellipodium.

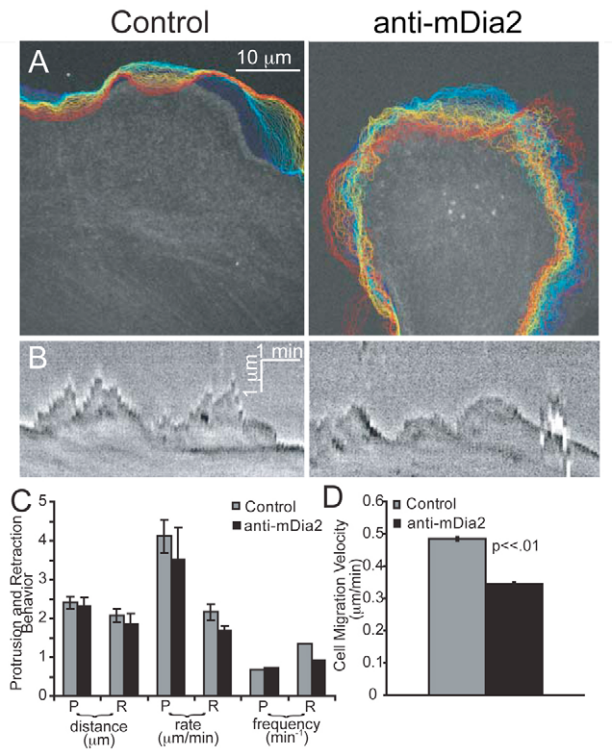

Fig. 7. mDia2 is necessary for concerted leading edge protrusions and retractions and rapid cell migration. (A) Control and mDia2 antibody-injected (anti-mDia2) cells were microinjected with X-Rhodamine actin and filmed by time-lapse spinning-disk confocal microscopy. Using qFSM software, the position of the cell edge was extracted from each image and are shown as changing from warm to cool colors over time. The edge of control cells are smooth and protrude and adjacent regions retract in a concerted fashion, whereas mDia2 antibody-injected cells displayed a much more ragged cell edge. (B) Kymographs taken from phase-contrast time-lapse images used to measure parameters of leading-edge dynamics. (C) The distance, rate and frequency of protrusions and retractions were not affected by mDia2 inhibition; n=10 cells per treatment, three measurements per cell. (D) The rate of PtK1 cell migration was significantly reduced by mDia2 inhibition, n=~30 cells per treatment.

mDia2 inhibition changes leading edge morphology and cell migration rates

Proper regulation of F-actin and focal adhesion dynamics are necessary for efficient epithelial cell migration. mDia2 antibody inhibition altered the dynamics and organization of both F-actin and focal adhesions, so we hypothesized that mDia2 function may be critical for epithelial cell migration. Since lamellipodium protrusion is the first step of migration, we analyzed parameters of leading edge behavior in migrating control and anti-mDia2 antibody-injected cells (Fig. 7). Tracking leading edge position over time from FSM movies (Fig. 7A) indicated that the leading edges of control cells were relatively smooth in contour and that their protrusions and retractions were coordinated along 5-10 μm lengths of the cell edge. By contrast, mDia2-inhibited cells displayed a more 'ragged' leading edge contour, with closely neighboring regions protruding and retracting independently. δFH2-expressing cells also displayed a ragged leading edge, indicative of uncoordinated protrusions and retractions (Fig. 3J,K). The uncoordinated protrusions and retractions and ragged edge contour may correspond to the frequent lack of a lamellipodium along the leading edge as determined by FSM of F-actin (Fig. 3C).

Although the smoothness (Fig. 7A) and stability (Fig. 4I) of the cell edge were affected by mDia2 inhibition, measurement of the dynamic parameters of leading edge protrusion and retraction by kymograph analysis (Fig. 7B) indicated that mDia2 inhibition did not alter the rate, distance or frequency of protrusion or retraction phases at any one point along the cell edge (Fig. 7C). This is similar to findings showing that mDia2 inhibition did not alter parameters of actin kinetics or kinematics in the lamellipodium (Fig. 3D,E), which probably mediate its protrusion and retraction behavior (Ponti et al., 2004).

To determine the role of mDia2 in cell motility, migration velocities of cells in small epithelial islands (two to six cells) were measured from time-lapse movies of cell islands containing either all control cells or all anti-mDia2 antibody-injected cells. This showed that the instantaneous velocity of anti-mDia2 antibody-injected cells was reduced by 30% compared with that of control cells (Fig. 7D, P<0.0001). In summary, mDia2 function is necessary for rapid epithelial cell migration and concerted leading edge protrusions and retractions, but not for the rate or distance of protrusion or retraction events.

Discussion

In this study we aimed to test the hypothesis that mammalian Diaphanous-related formins (DRFs) spatially and temporally regulate the dynamics of specific F-actin-based structures, the lamellipodium and lamella, in migrating epithelial cells, and to determine whether this mDia-mediated regulation of F-actin behavior is critical for cell migration. To test this hypothesis, we inhibited the major DRF expressed in PtK1 cells, mDia2, by microinjection of a polyclonal antibody that specifically blocks mDia2-mediated actin polymerization in vitro or overexpression of a dominant-negative mDia2 protein. Consistent with our hypothesis, we found that mDia2 inhibition not only affected the organization and dynamics of specific F-actin structures within the cell, but also affected the dynamics and organization of focal adhesions and slowed cell migration. Although these effects are probably attributable to mDia2's role in regulating F-actin assembly kinetics, we cannot rule out that other functions of mDia2 or other DRFs are affected by our perturbations in PtK1 cells.

We found that mDia2 localizes to the lamella and central region of PtK1 cells in a filamentous and vesicular pattern that was partially overlapping with microtubules, but it was excluded from the lamellipodium F-actin network. Although mDia2 has been shown to regulate the formation of stable microtubules marked by their detyrosination (Palazzo et al., 2001), the injected mDia2 antibody had no effect on the quantity or distribution of detyrosinated microtubules in PtK1 cells (immunofluorescence analysis, data not shown). This suggests that microtubule stability may be regulated by regions of mDia2 that lie outside the FH2 domain against which our antibodies were raised.

Consistent with its localization within the lamella and absence from the lamellipodium, mDia2 inhibition by antibody

microinjection promoted specific effects on the rate of turnover of cortical F-actin in the lamella, as measured by TIR-FRAP. In the lamellipodium, mDia2 inhibition did not affect F-actin behavior, which consisted of a single population of dynamic F-actin that turned over quite rapidly. In the lamella, mDia2 was necessary for both maintaining a stable F-actin pool and for slowing the turnover of a dynamic pool. In vitro studies have shown that mDia2 increases the rate of both F-actin nucleation and elongation in the presence of profilin, while it retards elongation in the absence of profilin (Kovar et al., 2006). Thus, the dynamic F-actin pool in the lamella could be stabilized by mDia2 if this pool is polymerized preferentially from profilin-free actin. Alternatively, mDia2 also slows the rate of F-actin depolymerization in vitro (Romero et al., 2004), a fact that has received less attention. Thus, one possible explanation for our data is that mDia2 stabilizes both the dynamic and stable pools of F-actin in the lamella by slowing or inhibiting filament depolymerization. It would also be interesting to determine the effects of mDia2 on F-actin dynamics in the central cell region where the protein also concentrated.

Using qFSM, we also found that mDia2 activity is necessary for the proper segregation of distinct lamellipodium and lamella F-actin kinematic and kinetic behaviors. In addition, TIR-FRAP revealed that mDia2 inhibition caused F-actin in the lamella region to adopt some characteristics of the lamellipodium, supporting the notion that these two actin networks can become merged. This was typified by loss of the stable lamella F-actin pool, and an increase in the rate of turnover of the dynamic pool of F-actin. The border between the lamellipodium and lamella is defined as the site of zero net F-actin polymerization, and spatially coincides with a negative F-actin flow speed gradient and the distal border of focal adhesions (Ponti et al., 2004; Hu et al., 2007). The mechanism underlying the segregation of F-actin networks could be explained if mDia2 imparts one kinetic behavior on F-actin in the lamella, while Arp2/3 and cofilin impart a different kinetic signature on F-actin in the lamellipodium (Hotulainen and Lappalainen, 2006; Ponti et al., 2004; Svitkina and Borisy, 1999). Interestingly, similar suggestions have been made for the lamella protein, tropomyosin (Bryce et al., 2003; DesMarais et al., 2002; Gupton et al., 2005). Alternatively, the segregation between the lamellipodium and lamella could be due to mDia2 function at focal adhesions, suggesting mDia2 mediates filament elongation specifically at these sites. We found that mDia2 inhibition resulted in the loss of polymerization-competent free barbed filament ends at focal adhesions. Whether or not actin polymerization occurs specifically at focal adhesions is unknown, but several recent studies have suggested this could be possible (Butler et al., 2006; DeMali et al., 2002; Hotulainen and Lappalainen, 2006). DRFs could act at focal adhesions via their recently revealed binding interaction with integrins (Butler et al., 2006) and could promote free barbed end formation or maintenance there either by new filament nucleation or inhibition of barbed end capping, both of which have been shown to be mediated by mDia2 in vitro. The growth/elongation of filaments from focal adhesions (Hotulainen and Lappalainen, 2006) could supply the lamella with either the stable or dynamic pools of F-actin. These filaments that are 'born' at focal adhesions in the lamella could be preferentially acted upon by activated myosin II that forms minifilaments also within the lamella (Verkhovsky et al., 1995). The action of myosin II on these filaments could drive the slower, myosin-dependent retrograde flow speed observed for lamella F-actin compared to the filaments in the lamellipodia that are moved much faster by polymerization-induced forces driven by Arp2/3 and cofilin activities (Ponti et al., 2004). This would result in segregation of F-actin flow speeds. Although mDia2 did not specifically localize to focal adhesions, it was not excluded from them. Identifying the location of activated mDia2 (versus total mDia2) in PtK1 cells could help to clarify this conundrum.

We additionally found that mDia2 is critical to focal adhesion turnover, as has recently been shown for the related mDia1 (Yamana et al., 2006). mDia2 antibody or dominant negative inhibition caused a buildup of focal adhesions across the lamella, probably via increasing lifetime, decreasing assembly and disassembly rates, and decreasing the rate of protein dissociation from focal adhesions. Since focal adhesion disassembly was most drastically affected, this probably induced the increased number of focal adhesions in the lamella. The lack of focal adhesion turnover is a possible culprit for the significant decrease in migration velocity following mDia2 inhibition, as has been suggested for cells after mDia1 depletion (Goulimari et al., 2005; Yamana et al., 2006). How DRFs regulate focal adhesion dynamics is unclear. Yamana et al. (Yamana et al., 2006) have evidence that mDia1 depletion impairs accumulation of active cSrc at focal adhesions which then attenuates Cas phosphorylation, suggesting a signaling role for mDia1 acting upstream of the Cas-Crk pathway that regulates focal adhesion turnover (Webb et al., 2004). As the antibodies used in our study were specific to an actin regulatory domain of mDia2, we suggest, as an alternative, that DRFs may play a mechanical role in focal adhesion turnover through their actin-nucleating/elongating activities. In PtK1 cells, perhaps mDia2-mediated filaments elongating at focal adhesions could modulate the amount of myosin II-generated force transmitted from these lamella filaments to focal adhesions, as myosin II-mediated force is known to promote both focal adhesion assembly and disassembly (Chrzanowska-Wodnicka and Burridge, 1996; Webb et al., 2004). mDia2 could relax the myosin II-mediated tension transmitted to focal adhesions by promoting actin polymerization at the focal adhesion that would 'feed' filaments to the myosin II that is pulling against the adhesion, reducing the force at the focal adhesion and allowing its dissolution. Since DRF activity has been shown to be required for force-induced focal adhesion maturation (Riveline et al., 2001), this suggests that force specifically on filaments 'born' at focal adhesions is a necessary step in the process of maturation and turnover. However, mDia2 has also been shown to affect the dynamics of microtubules (Palazzo et al., 2001; Wen et al., 2004), and other studies have found that microtubule targeting of focal adhesions is associated with focal adhesion disassembly (Kaverina et al., 1999; Palazzo et al., 2004). Since we found endogenous mDia2 along microtubules in PtK1 cells, it is possible that mDia2 could be the hypothesized 'relaxing factor' delivered to focal adhesions by microtubules to regulate their disassembly (Kaverina et al., 1999), although others have suggested that dynamin may play this role (Ezratty et al., 2005).

The effects of mDia2 inhibition on the lamellipodium that

we observed are at first confusing. We show that mDia2 inhibition has no effect on lamellipodium F-actin by several assays. These include (1) the rate of F-actin turnover as measured by TIR-FRAP; (2) the accumulation of polymerization-competent free filament barbed ends along the leading edge as measured by barbed-end localization; and (3) the speed of fast lamellipodial F-actin retrograde flow as measured by qFSM. In addition, mDia2 inhibition had no effect on leading edge protrusion and retraction parameters, which are mediated by lamellipodia F-actin dynamics (Ponti et al., 2004). However, by contrast, we also found by qFSM that mDia2 inhibition blocked the formation of the lamellipodium at discrete sites along the cell edge, which probably resulted in the jagged leading edge contour and loss of coordination of concerted protrusions and retractions along the leading edge also seen in cells with perturbed mDia2 function. Although mDia2 could also play a role in regulating F-actin dynamics in the lamellipodium that we did not uncover here, we suggest that the effects of mDia2 inhibition on lamellipodial behavior that we observed may be indirect. Previous studies have found that the distinct networks of the lamellipodium and lamella of migrating epithelial cells are often spatially overlapping (Ponti et al., 2004). This suggests that lamella F-actin may provide a stable 'platform' for the dynamic cycles of lamellipodial protrusion and retraction, by perhaps providing 'mother' filaments on which Arp2/3-mediated filament nucleation mediates the formation of a branched filament network. Thus, the existence of the lamellipodium would be dependent on a local source of stable mother filaments from the lamella. Since mDia2 inhibition destabilized filaments in the lamella, this could explain the spatially and temporally local loss of the lamellipodium at sites along the leading edge.

In conclusion, we have shown that mDia2 is intimately involved in the proper organization and dynamics of F-actin in the lamella, the turnover of focal adhesions, and the stability of the lamellipodium. Since these are integral factors of cell migration, it is not surprising that inhibition of mDia2 significantly slowed cell migration. These data further support the hypothesis that the lamella powers cell migration in epithelial cells, as mDia2 inhibition altered many parameters of actin behavior in this region of the cell.

Materials and Methods

Antibodies

Polyclonal anti-mDia2 antibodies were made by immunizing rabbits with purified recombinant mDia2 protein (amino acids 501-1141) made in bacteria (Wallar et al., 2007). The resulting antiserum (1358) was affinity-purified against GST-mDia2 fusion protein using standard procedures. Anti-mDia1 antibody was described previously (Tominaga et al., 2000). Anti-mDia3 rabbit polyclonal antibodies were generated against the C-terminal fragment of human mDia3 (also known as DIAPH1; a.a. 1078-1093). Paxillin antibodies were obtained from Signal Transduction Laboratories. Tubulin antibody DM1A was obtained from Sigma.

Immunoblotting

HEK 293T and HeLa cells were maintained in DMEM containing 10% (v/v) fetal bovine serum (FBS). PtK1 (rat kangaroo kidney epithelial) cells were maintained in F12 medium (Sigma) with 10% fetal bovine serum (Gibco). Transfection of HEK 293T was performed using Lipofectamine 2000 with OptiMEM (Invitrogen) according to the manufacturer's specifications. After 18 hours of transfection, cell lysates were prepared in lysis buffer (20 mM Tris-HCl, pH 7.5, 100 mM NaCl, 1% NP40, 10% glycerol) containing 0.1 M each sodium vanadate, aprotinin, pepstatin, leupeptin, dithiothreitol and PMSF, and immunoprecipitations were performed as previously described (Tominaga et al., 2000). Alternatively, whole lysates were prepared by washing cells in ice cold PBS, followed by addition of SDS sample buffer. Cell lysates were boiled for 10 minutes and protein concentrations quantified. Equal protein concentrations of cell lysates were loaded into gels.

Cell culture and microinjection

PtK1 cells were plated in F12 medium (Sigma) with 10% fetal bovine serum (Gibco) on #1.5 coverslips. For antibody inhibition, cells were microinjected with 0.1 mg/ml affinity purified antibody in PBS. For dominant negative mDia2 perturbation, expression plasmid encoding mutant cDNA were co-microinjected with labeled actin into the nucleus (Gupton et al., 2005). To visualize F-actin or adhesion dynamics in inhibited cells, antibody was mixed with X-Rhodamine-conjugated actin and/or plasmid DNA as described previously (Gupton et al., 2005) prior to microinjection. Control cells were injected with fluorescent actin or DNA alone. Cells were prepared for live cell microscopy as described previously (Gupton et al., 2005).

Immunofluorescence and quantification of polymerization-competent free barbed ends

Cells were fixed with either –20°C methanol or paraformaldehyde and processed for immunofluorescence as described previously (Gupton et al., 2005), using Cy2 secondary antibodies (Jackson Research) and Alexa Fluor 568 phalloidin (Molecular Probes) for staining F-actin. To localize and quantify the relative number of F-actin free barbed ends, live cells were permeabilized with 0.25 mg/ml saponin in the presence of 0.5 μM X-Rhodamine actin and fixed as previously described (Symons and Mitchison, 1991).

Microscopy

Fluorescent speckle microscopy (FSM) and phase-contrast time-lapse image series of F-actin were acquired at 5- to 10-second intervals using a 100× 1.4 NA Plan APO phase-contrast objective lens (Nikon) on a CSU-10 (Yokogawa) spinning-disk confocal digital microscope system (Adams et al., 2003). GFP-paxillin images were acquired at 15-second intervals using the same system. Leading edge activity and cell migration rates were determined from phase-contrast time series acquired on the inverted microscope system described by de Rooij et al. (de Rooij et al., 2005) using a 20× 0.5 NA Plan Apo objective lens (Nikon). For cell velocity, images of small islands of two to six cells were captured at 2-minute intervals for 16 hours; for leading edge characterization, images were obtained at 10-second intervals for 10 minutes. Islands were composed completely of either control cells or mDia2 antibody-injected cells. Epifluorescence images of fixed cells were acquired on an inverted microscope system (Wittmann et al., 2003) using a 60× 1.4 NA plan Apo DIC objective lens (Nikon). Fluorescence recovery after photobleaching (FRAP) was performed on a Nikon TE2000-U with a custom built fiber-optic coupled epi-illuminator for through-the-objective total internal reflection fluorescence (TIRF) illumination using a 100× 1.45 NA TIRF DIC objective lens (Nikon) with an OrcaERII (Hamamatsu) camera. Laser illumination at 488 or 568 nm was selected from a coherent Innova 70C Spectrum 2.5 W Kr/Ar laser using a polychromatic accousto-optic modulator (PCAOM) with an 8 channel driver (Neos Technologies). Light delivery to the epi-illuminator was through an Oz optics fiber optic cable. Actin or focal adhesions were bleached by using the laser at full power with the TIRF evanescent field adjusted to ~150 nm from the coverslip surface; recovery of fluorescence was imaged at 0.5-5 second intervals for 20 minutes using laser light significantly attenuated by the PCAOM.

Image analysis

Parameters of leading edge behavior and cell migration velocity were analyzed as described previously (Gupton et al., 2005). F-actin flow rates were measured by kymograph analysis (Salmon et al., 2002), flow maps were produced with qFSM software (Ponti et al., 2004). The lamellipodium-lamella border was delineated by a negative flow-speed gradient, the lamella was delineated by boundaries with the lamellipodium and the convergence zone (Salmon et al., 2002).

To compare the gradient of F-actin retrograde flow among control and mDia2-inhibited cells, the speed of F-actin flow in each cell was averaged in intervals based on distance from the cell edge. The cell boundary was extracted from fluorescence images as described (Machacek and Danuser, 2006). F-actin flow speed at all points in the cell, as determined by qFSM, was averaged parallel to the cell edge in 1-μm intervals behind the cell edge for five control and five anti-mDia2-antibody injected cells. The averages of these data were plotted versus distance from the cell edge.

F-actin polymerization and depolymerization maps were calculated using qFSM software (Ponti et al., 2003; Vallotton et al., 2003). Quantification of focal adhesion dynamics was performed for image series of GFP-paxillin as described (Webb et al., 2004). For analysis of photobleaching recovery, the integrated fluorescence intensity was recorded in pre-bleach and recovery image series. Calculations of the percentage of recovery and $t_{1/2}$ of recovery was performed as described previously (Bulinski et al., 2001). Focal adhesion number, density and size were counted using Metamorph software as described previously (Gupton and Waterman-Storer, 2006b).

Statistical analysis

When data were normally distributed, statistical differences between control and mDia2-inhibited cells were determined using independent sample t-tests with unequal variance. When data were not normally distributed, we compared data using nonparametric Mann-Whitney tests to determine statistical significance. *P*-values

derived from *t*-tests are included in the text without description, whereas *P*-values derived using the Mann-Whitney comparison are indicated in the text.

We thank Harry Higgs and Elizabeth Harris for insightful discussions and for sharing unpublished data with us, Ana Maria Pasapera-Limon for preparation of PtK lysates, Matthias Machacek for help with cell edge tracking, Lin Ji for help with comparing actin speed gradients, also Bill Shin for care of the microscopes, and the Gertler Lab for support in finishing final experiments. C.M.W.S. is an Established Investigator of the American Heart Association (0640086N), a recipient of the NIH Director's Pioneer Award (OD000435) and is supported by NIH GM67230. A.S.A. is supported by the Van Andel Foundation, the NIH (CA107529) and the American Cancer Society (RSG-05-033-01-CSM). K.E. is supported by an NRSA postdoctoral fellowship (F32 GM723313) and S.L.G. is an HHMI pre-doctoral fellow.

References

Adams, M. C., Salmon, W. C., Gupton, S. L., Cohan, C. S., Wittmann, T., Prigozhina, N. and Waterman-Storer, C. M. (2003). A high-speed multispectral spinning-disk confocal microscope system for fluorescent speckle microscopy of living cells. *Methods* **29**, 29-41.

Arnaout, M. A. (2002). Integrin structure: new twists and turns in dynamic cell adhesion. *Immunol. Rev.* **186**, 125-140.

Bailly, M., Macaluso, F., Cammer, M., Chan, A., Segall, J. E. and Condeelis, J. S. (1999). Relationship between Arp2/3 complex and the barbed ends of actin filaments at the leading edge of carcinoma cells after epidermal growth factor stimulation. *J. Cell Biol.* **145**, 331-345.

Bryce, N. S., Schevzov, G., Ferguson, V., Percival, J. M., Lin, J. J., Matsumura, F., Bamburg, J. R., Jeffrey, P. L., Hardeman, E. C., Gunning, P. et al. (2003). Specification of actin filament function and molecular composition by tropomyosin isoforms. *Mol. Biol. Cell* **14**, 1002-1016.

Bulinski, J. C., Odde, D. J., Howell, B. J., Salmon, T. D. and Waterman-Storer, C. M. (2001). Rapid dynamics of the microtubule binding of ensconsin in vivo. *J. Cell Sci.* **114**, 3885-3897.

Butler, B., Gao, C., Mersich, A. T. and Blystone, S. D. (2006). Purified integrin adhesion complexes exhibit actin-polymerization activity. *Curr. Biol.* **16**, 242-251.

Chrzanowska-Wodnicka, M. and Burridge, K. (1996). Rho-stimulated contractility drives the formation of stress fibers and focal adhesions. *J. Cell Biol.* **133**, 1403-1415.

Copeland, J. W. and Treisman, R. (2002). The diaphanous-related formin mDia1 controls serum response factor activity through its effects on actin polymerization. *Mol. Biol. Cell* **13**, 4088-4099.

Copeland, J. W., Copeland, S. J. and Treisman, R. (2004). Homo-oligomerization is essential for F-actin assembly by the formin family FH2 domain. *J. Biol. Chem.* **279**, 50250-50256.

Critchley, D. R., Holt, M. R., Barry, S. T., Priddle, H., Hemmings, L. and Norman, J. (1999). Integrin-mediated cell adhesion: the cytoskeletal connection. *Biochem. Soc. Symp.* **65**, 79-99.

Danuser, G. and Waterman-Storer, C. M. (2003). Quantitative fluorescent speckle microscopy: where it came from and where it is going. *J. Microsc.* **211**, 191-207.

de Rooij, J., Kerstens, A., Danuser, G., Schwartz, M. A. and Waterman-Storer, C. M. (2005). Integrin-dependent actomyosin contraction regulates epithelial cell scattering. *J. Cell Biol.* **171**, 153-164.

DeMali, K. A., Barlow, C. A. and Burridge, K. (2002). Recruitment of the Arp2/3 complex to vinculin: coupling membrane protrusion to matrix adhesion. *J. Cell Biol.* **159**, 881-891.

DesMarais, V., Ichetovkin, I., Condeelis, J. and Hitchcock-DeGregori, S. E. (2002). Spatial regulation of actin dynamics: a tropomyosin-free, actin-rich compartment at the leading edge. *J. Cell Sci.* **115**, 4649-4660.

Di Nardo, A., Cicchetti, G., Falet, H., Hartwig, J. H., Stossel, T. P. and Kwiatkowski, D. J. (2005). Arp2/3 complex-deficient mouse fibroblasts are viable and have normal leading-edge actin structure and function. *Proc. Natl. Acad. Sci. USA* **102**, 16263-16268.

Eisenmann, K. M., Peng, J., Wallar, B. J. and Alberts, A. S. (2005). Rho GTPase-formin pairs in cytoskeletal remodelling. *Novartis Found. Symp.* **269**, 206-218; discussion 219-230.

Ezratty, E. J., Partridge, M. A. and Gundersen, G. G. (2005). Microtubule-induced focal adhesion disassembly is mediated by dynamin and focal adhesion kinase. *Nat. Cell Biol.* **7**, 581-590.

Gasman, S., Kalaidzidis, Y. and Zerial, M. (2003). RhoD regulates endosome dynamics through Diaphanous-related Formin and Src tyrosine kinase. *Nat. Cell Biol.* **5**, 195-204.

Goulimari, P., Kitzing, T. M., Knieling, H., Brandt, D. T., Offermanns, S. and Grosse, R. (2005). Galpha12/13 is essential for directed cell migration and localized Rho-Dia1 function. *J. Biol. Chem.* **280**, 42242-42251.

Gupton, S. L. and Waterman-Storer, C. M. (2006a). Live-cell fluorescent speckle microscopy of actin cytoskeleton dynamics and their perturbation by drug perfusion. In *Cell Biology: A Laboratory Handbook* (ed. J. E. Celis and J. V. Small), pp. 137-151. San Diego: Elsevier.

Gupton, S. L. and Waterman-Storer, C. M. (2006b). Spatiotemporal feedback between actomyosin and focal-adhesion systems optimizes rapid cell migration. *Cell* **125**, 1361-1374.

Gupton, S. L., Anderson, K. L., Kole, T. P., Fischer, R. S., Ponti, A., Hitchcock-DeGregori, S. E., Danuser, G., Fowler, V. M., Wirtz, D., Hanein, D. et al. (2005). Cell migration without a lamellipodium: translation of actin dynamics into cell movement mediated by tropomyosin. *J. Cell Biol.* **168**, 619-631.

Harris, E. S. and Higgs, H. N. (2006). Biochemical analysis of mammalian formin effects on actin dynamics. *Meth. Enzymol.* **406**, 190-214.

Harris, E. S., Li, F. and Higgs, H. N. (2004). The mouse formin, FRLalpha, slows actin filament barbed end elongation, competes with capping protein, accelerates polymerization from monomers, and severs filaments. *J. Biol. Chem.* **279**, 20076-20087.

Harris, E. S., Rouiller, I., Hanein, D. and Higgs, H. N. (2006). Mechanistic differences in actin bundling activity of two mammalian formins, FRL1 and mDia2. *J. Biol. Chem.* **281**, 14383-14392.

Higashida, C., Miyoshi, T., Fujita, A., Oceguera-Yanez, F., Monypenny, J., Andou, Y., Narumiya, S. and Watanabe, N. (2004). Actin polymerization-driven molecular movement of mDia1 in living cells. *Science* **303**, 2007-2010.

Higgs, H. N. and Peterson, K. J. (2005). Phylogenetic analysis of the formin homology 2 domain. *Mol. Biol. Cell* **16**, 1-13.

Hotulainen, P. and Lappalainen, P. (2006). Stress fibers are generated by two distinct actin assembly mechanisms in motile cells. *J. Cell Biol.* **173**, 383-394.

Hu, K., Ji, L., Applegate, K. T., Danuser, G. and Waterman-Storer, C. M. (2007). Differential transmission of actin motion within focal adhesions. *Science* **315**, 111-115.

Ichetovkin, I., Grant, W. and Condeelis, J. (2002). Cofilin produces newly polymerized actin filaments that are preferred for dendritic nucleation by the Arp2/3 complex. *Curr. Biol.* **12**, 79-84.

Kaverina, I., Krylyshkina, O. and Small, J. V. (1999). Microtubule targeting of substrate contacts promotes their relaxation and dissociation. *J. Cell Biol.* **146**, 1033-1044.

Kaverina, I., Krylyshkina, O. and Small, J. V. (2002). Regulation of substrate adhesion dynamics during cell motility. *Int. J. Biochem. Cell Biol.* **34**, 746-761.

Kovar, D. R. and Pollard, T. D. (2004). Insertional assembly of actin filament barbed ends in association with formins produces piconewton forces. *Proc. Natl. Acad. Sci. USA* **101**, 14725-14730.

Kovar, D. R., Wu, J. Q. and Pollard, T. D. (2005). Profilin-mediated competition between capping protein and formin Cdc12p during cytokinesis in fission yeast. *Mol. Biol. Cell* **16**, 2313-2324.

Kovar, D. R., Harris, E. S., Mahaffy, R., Higgs, H. N. and Pollard, T. D. (2006). Control of the assembly of ATP- and ADP-actin by formins and profilin. *Cell* **124**, 423-435.

Lauffenburger, D. A. and Horwitz, A. F. (1996). Cell migration: a physically integrated molecular process. *Cell* **84**, 359-369.

Laukaitis, C. M., Webb, D. J., Donais, K. and Horwitz, A. F. (2001). Differential dynamics of alpha 5 integrin, paxillin, and alpha-actinin during formation and disassembly of adhesions in migrating cells. *J. Cell Biol.* **153**, 1427-1440.

Machacek, M. and Danuser, G. (2006). Morphodynamic profiling of protrusion phenotypes. *Biophys. J.* **90**, 1439-1452.

Michelot, A., Guerin, C., Huang, S., Ingouff, M., Richard, S., Rodiuc, N., Staiger, C. J. and Blanchoin, L. (2005). The formin homology 1 domain modulates the actin nucleation and bundling activity of Arabidopsis FORMIN1. *Plant Cell* **17**, 2296-2313.

Moseley, J. B., Sagot, I., Manning, A. L., Xu, Y., Eck, M. J., Pellman, D. and Goode, B. L. (2004). A conserved mechanism for Bni1- and mDia1-induced actin assembly and dual regulation of Bni1 by Bud6 and profilin. *Mol. Biol. Cell* **15**, 896-907.

Palazzo, A. F., Cook, T. A., Alberts, A. S. and Gundersen, G. G. (2001). mDia mediates Rho-regulated formation and orientation of stable microtubules. *Nat. Cell Biol.* **3**, 723-729.

Palazzo, A. F., Eng, C. H., Schlaepfer, D. D., Marcantonio, E. E. and Gundersen, G. G. (2004). Localized stabilization of microtubules by integrin- and FAK-facilitated Rho signaling. *Science* **303**, 836-839.

Pankov, R., Endo, Y., Even-Ram, S., Araki, M., Clark, K., Cukierman, E., Matsumoto, K. and Yamada, K. M. (2005). A Rac switch regulates random versus directionally persistent cell migration. *J. Cell Biol.* **170**, 793-802.

Peng, J., Wallar, B. J., Flanders, A., Swiatek, P. J. and Alberts, A. S. (2003). Disruption of the Diaphanous-related formin Drf1 gene encoding mDia1 reveals a role for Drf3 as an effector for Cdc42. *Curr. Biol.* **13**, 534-545.

Pollard, T. D. and Borisy, G. G. (2003). Cellular motility driven by assembly and disassembly of actin filaments. *Cell* **112**, 453-465.

Ponti, A., Vallotton, P., Salmon, W. C., Waterman-Storer, C. M. and Danuser, G. (2003). Computational analysis of F-actin turnover in cortical actin meshworks using fluorescent speckle microscopy. *Biophys. J.* **84**, 3336-3352.

Ponti, A., Machacek, M., Gupton, S. L., Waterman-Storer, C. M. and Danuser, G. (2004). Two distinct actin networks drive the protrusion of migrating cells. *Science* **305**, 1782-1786.

Ponti, A., Matov, A., Adams, M., Gupton, S., Waterman-Storer, C. M. and Danuser, G. (2005). Periodic patterns of actin turnover in lamellipodia and lamellae of migrating epithelial cells analyzed by quantitative fluorescent speckle microscopy. *Biophys. J.* **89**, 3456-3469.

Pruyne, D., Evangelista, M., Yang, C., Bi, E., Zigmond, S., Bretscher, A. and Boone, C. (2002). Role of formins in actin assembly: nucleation and barbed-end association. *Science* **297**, 612-615.

Ridley, A. J. (2006). Rho GTPases and actin dynamics in membrane protrusions and vesicle trafficking. *Trends Cell Biol.* **16**, 522-529.

Riveline, D., Zamir, E., Balaban, N. Q., Schwarz, U. S., Ishizaki, T., Narumiya, S., Kam, Z., Geiger, B. and Bershadsky, A. D. (2001). Focal contacts as mechanosensors: externally applied local mechanical force induces growth of focal contacts by an mDia1-dependent and ROCK-independent mechanism. *J. Cell Biol.* **153**, 1175-1186.

Romero, S., Le Clainche, C., Didry, D., Egile, C., Pantaloni, D. and Carlier, M. F. (2004). Formin is a processive motor that requires profilin to accelerate actin assembly and associated ATP hydrolysis. *Cell* **119**, 419-429.

Salmon, W. C., Adams, M. C. and Waterman-Storer, C. M. (2002). Dual-wavelength fluorescent speckle microscopy reveals coupling of microtubule and actin movements in migrating cells. *J. Cell Biol.* **158**, 31-37.

Sund, S. E. and Axelrod, D. (2000). Actin dynamics at the living cell submembrane imaged by total internal reflection fluorescence photobleaching. *Biophys. J.* **79**, 1655-1669.

Svitkina, T. M. and Borisy, G. G. (1999). Arp2/3 complex and actin depolymerizing factor/cofilin in dendritic organization and treadmilling of actin filament array in lamellipodia. *J. Cell Biol.* **145**, 1009-1026.

Symons, M. H. and Mitchison, T. J. (1991). Control of actin polymerization in live and permeabilized fibroblasts. *J. Cell Biol.* **114**, 503-513.

Tominaga, T., Sahai, E., Chardin, P., McCormick, F., Courtneidge, S. A. and Alberts, A. S. (2000). Diaphanous-related formins bridge Rho GTPase and Src tyrosine kinase signaling. *Mol. Cell* **5**, 13-25.

Vallotton, P., Ponti, A., Waterman-Storer, C. M., Salmon, E. D. and Danuser, G. (2003). Recovery, visualization, and analysis of actin and tubulin polymer flow in live cells: a fluorescent speckle microscopy study. *Biophys. J.* **85**, 1289-1306.

Verkhovsky, A. B., Svitkina, T. M. and Borisy, G. G. (1995). Myosin II filament assemblies in the active lamella of fibroblasts: their morphogenesis and role in the formation of actin filament bundles. *J. Cell Biol.* **131**, 989-1002.

Wallar, B. J., Deward, A. D., Resau, J. H. and Alberts, A. S. (2007). RhoB and the mammalian Diaphanous-related formin mDia2 in endosome trafficking. *Exp. Cell Res.* **313**, 560-571.

Watanabe, N., Kato, T., Fujita, A., Ishizaki, T. and Narumiya, S. (1999). Cooperation between mDia1 and ROCK in Rho-induced actin reorganization. *Nat. Cell Biol.* **1**, 136-143.

Webb, D. J., Donais, K., Whitmore, L. A., Thomas, S. M., Turner, C. E., Parsons, J. T. and Horwitz, A. F. (2004). FAK-Src signalling through paxillin, ERK and MLCK regulates adhesion disassembly. *Nat. Cell Biol.* **6**, 154-161.

Wen, Y., Eng, C. H., Schmoranzer, J., Cabrera-Poch, N., Morris, E. J., Chen, M., Wallar, B. J., Alberts, A. S. and Gundersen, G. G. (2004). EB1 and APC bind to mDia to stabilize microtubules downstream of Rho and promote cell migration. *Nat. Cell Biol.* **6**, 820-830.

Wheeler, A. P., Wells, C. M., Smith, S. D., Vega, F. M., Henderson, R. B., Tybulewicz, V. L. and Ridley, A. J. (2006). Rac1 and Rac2 regulate macrophage morphology but are not essential for migration. *J. Cell Sci.* **119**, 2749-2757.

Wittmann, T., Bokoch, G. M. and Waterman-Storer, C. M. (2003). Regulation of leading edge microtubule and actin dynamics downstream of Rac1. *J. Cell Biol.* **161**, 845-851.

Yamana, N., Arakawa, Y., Nishino, T., Kurokawa, K., Tanji, M., Itoh, R. E., Monypenny, J., Ishizaki, T., Bito, H., Nozaki, K. et al. (2006). The Rho-mDia1 pathway regulates cell polarity and focal adhesion turnover in migrating cells through mobilizing Apc and c-Src. *Mol. Cell. Biol.* **26**, 6844-6858.

Yasuda, S., Oceguera-Yanez, F., Kato, T., Okamoto, M., Yonemura, S., Terada, Y., Ishizaki, T. and Narumiya, S. (2004). Cdc42 and mDia3 regulate microtubule attachment to kinetochores. *Nature* **428**, 767-771.

Zaidel-Bar, R., Ballestrem, C., Kam, Z. and Geiger, B. (2003). Early molecular events in the assembly of matrix adhesions at the leading edge of migrating cells. *J. Cell Sci.* **116**, 4605-4613.

Zigmond, S. H., Evangelista, M., Boone, C., Yang, C., Dar, A. C., Sicheri, F., Forkey, J. and Pring, M. (2003). Formin leaky cap allows elongation in the presence of tight capping proteins. *Curr. Biol.* **13**, 1820-1823.

Zimerman, B., Volberg, T. and Geiger, B. (2004). Early molecular events in the assembly of the focal adhesion-stress fiber complex during fibroblast spreading. *Cell Motil. Cytoskeleton* **58**, 143-159.